Dielectric spectroscopy on the quasi–one-dimensional organic charge density wave conductor (Fluoranthene)2PF6

C. Math, Wolfgang Brütting, W. Rieß

Angaben zur Veröffentlichung / Publication details:

Math, C., Wolfgang Brütting, and W. Rieß. 1996. "Dielectric spectroscopy on the quasi–one-dimensional organic charge density wave conductor (Fluoranthene)2PF6." *Europhysics Letters (EPL)* 35 (3): 221–26. https://doi.org/10.1209/epl/i1996-00558-3.

Dielectric spectroscopy on the quasi–one-dimensional organic charge density wave conductor (Fluoranthene)$_2$PF$_6$

C. Math[1], W. Brütting[1] and W. Rieß[2]

[1] *Physikalisches Institut und Bayreuther Institut für Makromolekülforschung Universität Bayreuth - D-95440 Bayreuth, Germany*
[2] *IBM Research Division, Zurich Research Laboratory CH-8803 Rüschlikon, Switzerland*

PACS. 71.45Lr – Charge-density-wave systems.
PACS. 72.15Nj – Collective modes (*e.g.*, in one-dimensional conductors).
PACS. 77.22Gm– Dielectric loss and relaxation.

Abstract. – Frequency-dependent complex conductivity measurements on the organic quasi–one-dimensional CDW system (Fa)$_2$PF$_6$ between 10^{-4} Hz and $3\cdot10^9$ Hz at temperatures ranging from 20 K to 290 K are reported. Below the temperature of the Peierls transition ($T_P = 182$ K) the real part of the conductivity exhibits two structures, which can be attributed to two modes of the charge density wave (CDW): a temperature-dependent low-frequency relaxational mode of local oscillating deformations and a high-frequency resonant mode of the pinned CDW as a whole. The measurements indicate that the damping of the relaxational mode is dominated by free carriers in the covered temperature range. At low temperatures the dynamics of the CDW in (Fa)$_2$PF$_6$ shows features characteristic of the transition into a glass-like state.

Introduction. – In recent years the electrodynamic properties of the charge density wave (CDW) state have intensely been studied on inorganic model systems like $K_{0.3}MoO_3$, $(TaSe_4)_2I$ and $NbSe_3$ [1]-[3]. The CDW ground state appears in many low-dimensional conductors below a specific temperature (Peierls temperature T_P) and is characterized by the condensation of electrons into a harmonic wave with period (π/k_F), combined with the distortion of the lattice with the same period and a single-particle energy gap 2Δ typically in the order of 100 meV. Frequency-dependent measurements in inorganic CDW systems revealed a number of excitations with energies below the single-particle gap. In the microwave-to-millimeter frequency range the conductivity exhibits a pronounced peak, whereas at radio frequencies the conductivity contribution of the CDW develops a low-frequency tail. At higher temperatures both features can be explained within the frame of the extended Fukuyama-Lee-Rice (FLR) theory, which takes into account the interaction of the phase with pinning centres and free electrons [4]-[6].

Recent investigations at low temperatures indicate that the dynamic behaviour of the CDW is more complex in this temperature regime than the physical picture described by calculations based on the extended FLR theory. Calorimetric measurements show that inorganic CDW systems at very low temperature reveal typical features of a glassy state, like low activation energies and very slow relaxational dynamics [7]. Further experimental evidence for a glassy behaviour has also been found by frequency-dependent conductivity measurements at low temperatures, where a critical slowing-down of the relaxation and the appearance of a second relaxational process were observed [8].

In this work we have extended earlier measurements [9] on the organic CDW system $(Fa)_2PF_6$ down to lower temperatures (20 K) and frequencies (10^{-4} Hz). $(Fa)_2PF_6$ is a radical cation salt based on the organic donor molecule fluoranthene (Fa), which is an aromatic hydrocarbon ($C_{16}H_{10}$). Due to the uniaxial crystal structure the anisotropy of the conductivity is high ($\sigma_\parallel/\sigma_\perp = 10^4$) and the material undergoes a metal-insulator transition (opening of a single-particle gap $2\Delta(0)$ with a typical value of 180 meV) into a CDW ground state at 182 K [10]. As detected by X-ray investigations, the lattice constant in chain direction in the CDW ground state is about two times the lattice constant (6.61 Å) in the state above T_P (close to commensurability), which can be accounted for by the half-filled conduction band [11]. As in inorganic compounds several collective transport phenomena in the CDW ground state of $(Fa)_2PF_6$ have been observed, *e.g.* nonlinear conductivity above a certain threshold field (about 0.5 V/cm) and broad-band noise [12]. The absence of narrow-band noise indicates that in contrast to most inorganic CDW conductors apart from defect pinning also commensurability pinning of the CDW with the underlying lattice plays a major role in CDW dynamics [12].

With our investigation we wanted to get a complete characterization of the dynamic behaviour of the CDW in $(Fa)_2PF_6$ down to lowest temperatures and frequencies that are accessible to the method of dielectric spectroscopy. Because of the described peculiarities of our system it is interesting to compare its low-temperature behaviour with the one of inorganic systems.

Experiment. – In dielectric spectroscopy one measures the frequency-dependent real and imaginary parts of the impedance $Z(\omega)$ of a substance put between two capacitor plates of cross-section A and distance l. From $Z(\omega)$ other dielectric quantities of interest, like the complex conductivity $\sigma(\omega)$ and the complex dielectric permittivity $\epsilon(\omega)$, can be derived by the standard equations $\sigma(\omega) = l/A \cdot 1/Z(\omega)$ and $\epsilon(\omega) = (\sigma(\omega) - \sigma_{DC})/i\omega\epsilon_0$ (σ_{DC}: DC conductivity arising solely from free electrons; ϵ_0: vacuum permittivity). In order to attain a full picture of a dielectric process it is necessary to analyse two complementary parts of these quantities. Usually these are the real and imaginary parts of the dielectric function $\epsilon(\omega)$. Because of the high DC conductivity of our samples, leading to an uncertainty in the determination of the imaginary part of the dielectric function at low frequencies, it seems useful in this case to look at the real part of the conductivity $\sigma'(\omega)$ and at the real part of the dielectric function $\epsilon'(\omega)$ to describe the dielectric behaviour.

Performing impedance measurements in the frequency range from 10^{-4} Hz to $3 \cdot 10^9$ Hz requires the application of different experimental techniques. In the low-frequency range from 10^{-4} Hz to 10^7 Hz we used a frequency response analyser (Schlumberger SI 1260) in combination with a broad-band dielectric converter (Novocontrol) as preamplifier. This set-up allows impedance measurements up to $10^{14}\,\Omega$ with a $\tan\delta$ resolution (= ratio of real-to-imaginary part of the impedance, which can be simultaneously measured) of 10^{-4} at best. In this frequency range the measurements were carried out in a two-probe configuration with the sample glued to gold wires (50 µm) with conductive carbon cement (Demetron). The samples had a typical length of some mm and a cross-section of 0.5 mm^2. Because of the high values for the dielectric constant of $(Fa)_2PF_6$ stray capacitances can be neglected in this configuration.

In the high-frequency range from 300 kHz to 3 GHz coaxial reflectometry was applied for measuring the impedance using a network-analyser (Hewlett Packard 8753C). With this measurement technique impedances between $10^{-2}\,\Omega$ and $10^5\,\Omega$ can be measured in our experiment with a $\tan\delta$ resolution of 10^{-3} at best. The sample was put between two capacitor plates made from platinum and mounted atop of a PC-7 plug (Suhner) at the end of a coaxial waveguide.

Because of the application of two different techniques, measurements over the whole frequency range could not be carried out on one and the same sample. The frequency overlap

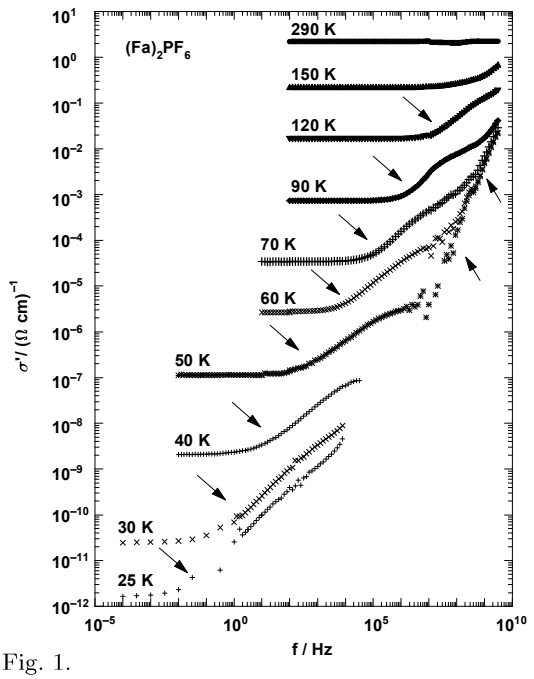

Fig. 1.

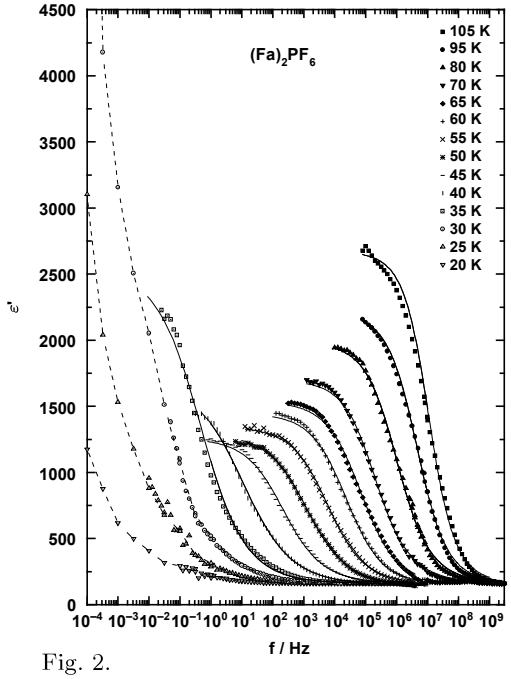

Fig. 2.

Fig. 1. – Real part σ' of the conductivity of $(Fa)_2PF_6$ for different temperatures exhibiting a strongly temperature-dependent low-frequency mode (↘) and the onset of a high-frequency mode (↖) below the Peierls transition at $T_P = 182\,K$.

Fig. 2. – Real part ϵ' of the complex dielectric function of $(Fa)_2PF_6$. Solid lines are fit curves with the Havriliak-Negami function, broken lines are guides to the eye.

between the two instruments and the use of samples from the same batch ensured that the results in the two frequency ranges could be put together consistently. The measurements were performed by cooling down the samples in 5 K steps in a continuous-flow cryostat (Oxford Instruments CF1200) with typical temperature stabilization times of 20 minutes. This procedure ensured that thermal hysteresis effects were absent. The sample temperature could be kept stable within 0.1 K throughout a frequency sweep. The electric field applied to the crystal was chosen small enough to avoid nonlinear conductivity effects.

The results for the real part of the conductivity of a $(Fa)_2PF_6$ sample at temperatures between 290 K and 25 K are shown in fig. 1. The frequency sweep was stopped at low frequencies when the $\tan\delta$ resolution was reached assuming that no further dielectric process occurs at even lower frequencies. At room temperature where $(Fa)_2PF_6$ is highly conducting (up to $1000\,(\Omega cm)^{-1}$)[12] the measured value of the impedance is limited by the contact resistance, which turns out to be frequency independent and rather small (typically about $5\,\Omega$). Below the Peierls transition (at 182 K) an onset (↘) for frequency-dependent behaviour appears at high frequencies (see, *e.g.*, the 150 K curve) and moves to lower frequencies with decreasing temperature. Below 90 K a second rise in the conductivity can be seen at high frequencies (↖). This second structure seems to be less temperature dependent, as all curves meet at high frequencies.

If one compares the structure of the conductivity curves with predictions of the extended FLR theory (see, *e.g.*, [6]), one finds a qualitative agreement between the measured behaviour and the model calculations. We therefore conclude that the low-frequency structure arises in the same way as in incommensurate systems from oscillating local deformations of the CDW,

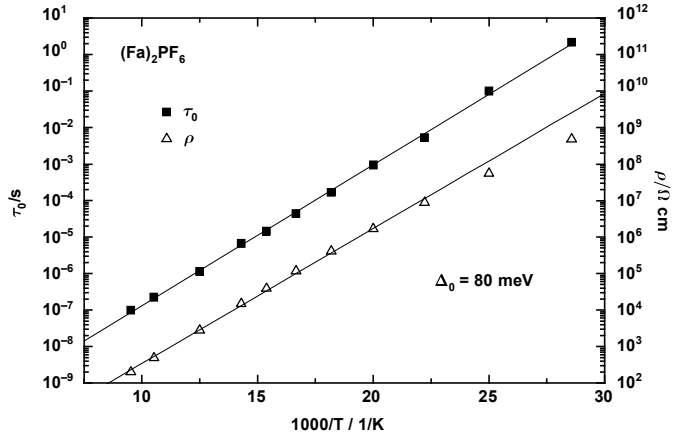

Fig. 3. – Temperature dependence of the mean relaxation time τ_0 and the specific dc resistance ρ in Arrhenius representation.

as assumed in this theory. The second rise at higher frequencies can be interpreted as the onset of a high-frequency conductivity peak arising from a transverse phason mode (pinned mode), which is to exist in the microwave region. Even though transverse modes couple to electromagnetic waves, they can show up in an experiment with only an electric field applied through mode mixing caused by a nonuniform pinning potential [4].

We used the following formula of the extended FLR theory to obtain a coarse estimation of the pinning frequency ω_0 at which the peak of the conductivity is expected to be:

$$\epsilon_{\mathrm{HF}} = \frac{n_{\mathrm{CDW}} e^2}{\epsilon_0 m^* \omega_0^2}\,; \tag{1}$$

ϵ_{HF} is the high-frequency dielectric constant of $\epsilon'(\omega)$ given by about 160 (see fig. 2). The CDW's effective mass m^* is given by

$$m^* = m_{\mathrm{e}}\Big(1 + \frac{4\Delta^2}{\lambda_0 \hbar^2 \omega_{2k_{\mathrm{F}}}^2}\Big) \tag{2}$$

and is about 2000 times the free-electron mass m_{e} using typical values for the gap 2Δ (180 meV), the dimensionless electron-phonon coupling constant λ_0 (0.3) and the phonon frequency $\omega_{2k_{\mathrm{F}}}$ ($10^{13}\,\mathrm{s}^{-1}$). From this we get a value of $7 \cdot 10^{11}$ Hz for $\omega_0/2\pi$. This value is much larger than our earlier estimation [9], which was based on the formula $\omega_0 \lambda_{\mathrm{p}} m^* = 2\pi e E_{\mathrm{T}}$ from the single-particle model [13] (λ_{p}: wavelength of pinning potential; E_{T}: threshold for nonlinear conduction). However, in a system close to commensurability nonlinear conductivity may arise already from the motion of local phase defects of the CDW (discommensurations) [14] rather than from a collective sliding of the CDW. Consequently, the threshold field E_{T} will not be related directly to ω_0 in our system. On the other hand, such a high value of the pinning frequency (in comparison with inorganic CDW systems) is not unexpected in the case of commensurability pinning.

As mentioned above, a more accurate description of the relaxational process can be obtained by analysing the real part $\epsilon'(\omega)$ of the dielectric function (fig. 2), which clearly displays the low-frequency Debye-like relaxational process of the CDW with ϵ' rising from a high-frequency value ϵ_{HF} to the static dielectric constant ϵ_{stat}.

A quantitative description of this behaviour can be obtained by fitting these curves with a

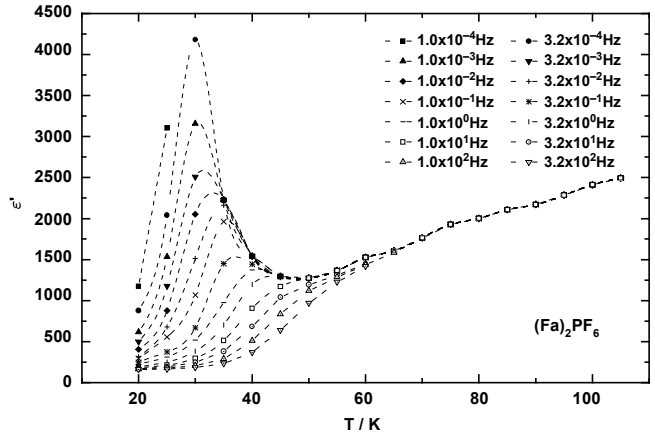

Fig. 4. – Temperature-dependent behaviour of the dielectric function ϵ' for different frequencies. For frequencies below 10 Hz a rise of the dielectric function leading to a maximum is observed (lines are guides to the eye).

generalized Debye function, *e.g.*, the Havriliak-Negami function:

$$\epsilon = \epsilon_{\mathrm{HF}} + \frac{\epsilon_{\mathrm{stat}} - \epsilon_{\mathrm{HF}}}{(1 + (i\omega\tau_0)^{(1-\alpha)})^{\beta}} \,. \tag{3}$$

For $\alpha = 0$ and $\beta = 1$ one gets the formula for the Debye curve which describes a relaxation of a system of noninteracting dipoles. The main parameter obtained by the analysis is the mean relaxation time τ_0, whose temperature dependence is shown in fig. 3. The Arrhenius plot reveals an activated behaviour of τ_0 and the resistivity $\rho = 1/\sigma_{\mathrm{DC}}$ over a large temperature range (105 K to 40 K) with an activation energy of 80 meV for both quantities.

The scaling of the relaxation time with the resistivity is in agreement with predictions of the extended FLR theory which are based on the assumption that local oscillating deformations of the CDW are damped by free-carrier currents. Thus, even though these models were devised for incommensurate systems, similar processes seem to be responsible for the relaxational behaviour in $(Fa)_2PF_6$, which has shown features of an almost commensurate system in earlier experiments [12]. The other parameters obtained by fitting the curves are α and β. The parameter α is a measure for the width of the relaxational curve and β for its skewness in comparison to the Debye curve. The values for β are in the order of 0.9 for all temperatures, which means that the relaxation is almost symmetric. The values of α increase from 0.25 to 0.5 with decreasing temperature reflecting the strong rise in the width of the relaxation (see fig. 2). This increasing deviation from the ideal Debye behaviour can be explained by a gradual freezing of the system in metastable states connected with a broadening of the distribution of the energy barriers between these states. In addition, the increase of the CDW's stiffness due to the reduced screening through free carriers at low temperatures leads to a higher interaction between the relaxing parts of the CDW and therefore to an increase of cooperative mechanisms.

A further parameter describing the delectric relaxation is the static dielectric constant ϵ_{stat}, which is in all CDW systems at least one order of magnitude larger than the high-frequency constant ϵ_{HF} and therefore serves as a measure for the strength of the relaxation process. ϵ_{stat} is in the order of 1000 for $(Fa)_2PF_6$ which is rather low if compared to ϵ_{stat} of systems like $K_{0.3}MoO_3$ and $(TaSe_4)_2I$, having values in the order of 10^6 and 10^5, respectively. We explain this difference by the dominance of the commensurability pinning mechanism that leads to a lower polarizability than in incommensurate systems, where impurity pinning dominates.

The static dielectric constant ϵ_{stat} at first decreases with decreasing temperature. As

indicated by the single-particle model ($\epsilon_{\mathrm{stat}} \cdot E_{\mathrm{T}} = \mathrm{const}$, see [13]) a correlation between ϵ_{stat} and the threshold field for nonlinear behaviour seems to exist in this temperature range (100 K to 40 K), because the observed threshold field usually increases at the same time [12]. At low temperatures (below 35 K) a strong rise in ϵ_{stat} is observed, leading to a maximum in the dielectric function if plotted against temperature for different frequencies (see fig. 4). A similar maximum has been detected in $K_{0.3}MoO_3$ and TaS_3 even though at higher temperatures and frequencies [8].

As in these materials the results for the dielectric behaviour at low temperature can be explained by the development of metastable states and an increase of cooperative mechanisms. Even though a second dielectric process or a slowing-down of τ_{r} described by a Vogel-Fulcher law ($\tau_{\mathrm{r}} = \tau_0 \exp[B/k(T - T_0)]$), which were observed in $K_{0.3}MoO_3$ [8] and which are typical for a glassy state, could not be detected, the behaviour at low temperatures shows features that have not been described in calculations of common models like the extended FLR theory and point to a transition into a glassy state. In a system close to commensurability a glassy state can arise from the presence of commensurate domains separated by discommensurations, where the phase of the CDW changes with respect to the lattice. The formation of these domains in a real system with impurities leads to many metastable states.

In conclusion, the organic CDW conductor $(Fa)_2PF_6$, which is a commensurate system as seen in earlier experiments, shows at higher temperatures a dynamic behaviour similar to inorganic systems, with a low-frequency relaxational mode and the onset of a high-frequency pinned mode, as described by the extended FLR theory. We have made an estimation for the pinning frequency ($7 \cdot 10^{11}$ Hz) using a result of the extended FLR theory. For confirming this estimation the investigations have to be extended to higher frequencies by performing microwave resonator and FTIR measurements. The dielectric relaxation at low temperatures showing features of a glassy state was investigated down to the lowest possible frequencies (10^{-4} Hz). To gain further insight into the behaviour at lower temperatures (< 20 K) other techniques like calorimetric measurements have to be applied in the future.

***

We thank G. Witt, A. Rötger and M. Schwoerer for helpful discussions and J. Gmeiner for growing the $(Fa)_2PF_6$ crystals. This work was supported by the Sonderforschungsbereich 279 and the Fonds der Chemischen Industrie.

REFERENCES

[1] Degiorgi L., Alavi B., Mihaly G. and Grüner G., *Phys. Rev. B*, **44** (1991) 7808.
[2] Cava R. J., Littlewood P., Fleming R. M., Dunn R. G. and Rietmann E. A., *Phys. Rev. B*, **33** (1986) 2439.
[3] Reagor D., Sridhar S. and Grüner G., *Phys. Rev. B*, **44** (1991) 7808.
[4] Littlewood P. B., *Phys. Rev. B*, **36** (1987) 3108.
[5] Baier T. and Wonneberger W., *Solid State Commun.*, **72** (1989) 773.
[6] Wonneberger W., *Synth. Met.*, **41-43** (1991) 3793.
[7] Biljakovic K., Lasjaunias J. C. and Monceau P., *J. Phys. IV*, **3**, C2 (1993) 335.
[8] Nad F. Ya. and Monceau P., *Solid State Commun.*, **87** (1993) 13.
[9] Brütting W., Witt G., Rötger A. and Rieß W., *Synth. Met.*, **70** (1995) 1303.
[10] Nguyen P. H., Paasch G., Brütting W. and Rieß W., *Phys. Rev. B*, **49** (1994) 5172; Brütting W., Nguyen P. H., Rieß W. and Paasch G., *Phys. Rev. B*, **51** (1995) 9533.
[11] Ilakovac V., Ravy S., Pouget J. P., Rieß W., Brütting W. and Schwoerer M., *J. Phys. IV*, **3**, C2 (1993) 137.
[12] Rieß W. and Brütting W., *Phys. Scr.*, **49** (1993) 721.
[13] Grüner G., Zawadowski A. and Chaikin P. M., *Phys. Rev. Lett.*, **46** (1981) 511.
[14] McMillan W. L., *Phys. Rev. B*, **14** (1976) 1496.